



PRZEMYSŁAW SKOTNICZNY*

**THREE-DIMENSIONAL NUMERICAL SIMULATION OF THE MASS EXCHANGE
BETWEEN LONGWALL HEADINGS AND GOAFs, IN THE PRESENCE OF METHANE DRAINAGE
IN A U-TYPE VENTILATED LONGWALL****SYMULACJA NUMERYCZNA 3D PROCESÓW WYMIANY MASY W UKŁADZIE WYROBISKA
ŚCIANOWE ZROBY, W ASPEKTCIE PROWADZENIA ODMETANOWANIA
ŚCIANY PRZEWIETRZANEJ SYSTEMEM NA „U”**

The phenomena related to the occurrence of methane in underground mines pose a considerable danger in the process of coal seam exploitation. Quite often, experimental analysis falls short of investigating their areas of origin (goafs area, affected rock mass, the tail gate area with abandoned excavation). Therefore, an invaluable tool for evaluating the risk involved in the exploitation process might be the numerical simulation of the phenomenon in question, carried out with the use of the latest CFD methods. Due to its application, we are able to recreate and predict the mechanism of the studied phenomenon, with certain assumptions and simplifications made.

The present paper discusses the results of the numerical simulation of the process of mass exchange occurring between affected rock mass and longwall headings. The calculations were performed for two test cases – 100 meter long walls.

Keywords: methane drainage, rock mass affected by mining exploitation, methane concentration in rock mass

Zjawiska związane z występowaniem metanu w kopalniach głębinowych stanowią poważne zagrożenie w procesie eksploatacji złóż węgla. Źródło występowania tych zjawisk dość często znajduje się poza możliwościami eksperymentalnej analizy (obszar zrobów, górotwór naruszony, strefa górnego naroża od strony zlikwidowanych wyrobisk ścianowych). Nieocenionym narzędziem oceny ryzyka eksploatacji w takim przypadku może stać się numeryczna symulacja zjawiska przy użyciu nowoczesnych metod CFD, która z uwzględnieniem pewnych założeń i uproszczeń jest w stanie odtworzyć oraz przewidzieć mechanizm zjawiska.

W prezentowanym artykule przedstawiono wyniki symulacji numerycznej procesu wymiany masy pomiędzy górotworem naruszonym eksploatacją a wyrobiskami ścianowymi. Obliczenia zostały przeprowadzone dla dwóch przypadków testowych (*test case*) 100 metrowej długości ścian.

Słowa kluczowe: odmetanowanie, górotwór naruszony eksploatacją, rozkład stężeń metanu w górotworze

* STRATA MECHANICS RESEARCH POLISH ACADEMY OF SCIENCES, UL. REYMONTA 27, 30-059 KRAKOW, POLAND

1. Introduction

Due to the fast development of the CFD (Computer Fluid Dynamics) methods, as well as more and more widespread access to efficient calculating machines, it is now possible to successfully determine flow parameters in cases which had previously posed serious difficulties, either because of a large computational domain or complex initial and boundary conditions (Dziurzyński et al., 2009; Fluent User..., 2011). The lion's share of the cases discussed here belong to the so-called environmental flow area, which includes large-scale flow phenomena.

Undoubtedly, all the phenomena related to the mass and energy exchange, occurring in underground mining facilities, are to be regarded as part of the area of environmental flows. In this case, the object for which determining the values of flow quantities becomes essential – for the sake of safety and efficiency of exploitation – is the complex ventilation network of underground headings, together with all the phenomena occurring there.

The exchange of mass and energy within the system: longwall headings – rock mass affected by exploitation, is one of the most important issues when it comes to the exploitation itself. Here, the basic safety indicator is the concentration of methane in longwall headings (Kozłowski & Grębski, 1982).

The results presented in this paper refer to the issue of the numerical simulation of the process of methane migration through rock mass, into the area of longwall headings. Additionally, the paper attempts to describe the process of the active methane drainage of the rock mass affected by exploitation. The solutions put forward here concern a specific test case, i.e. a 100 meter long longwall, which served as a basis for verifying the accuracy of the adopted boundary and initial conditions.

The mining practice shows that it is the most difficult to drain these walls which are ventilated by means of the U-type system. Thus, the present paper discusses the processes involved in ventilating such walls.

2. The project assumptions

The model of the wall, together with the area within rock mass, was designed according to the guidelines included in Instruction No. 14 issued by the Central Mining Institute (Krause & Łukowicz, 2000) and specifications from some other scientific publications (Kozłowski, 1972; Łukowicz, 2012). Fig. 1 presents a schematic diagram of the wall and the affected rock mass.

From the perspective of mass exchange between the affected rock mass and longwall headings, the most interesting areas are the ones marked I and II (Fig. 1), where the occurrence of tensile stresses results in increased fracturing of rock mass (the emergence of macropores). This facilitates the migration of the air and methane mix from the area of the relaxed rock mass. At the same time, due to the ventilation issues, the least advantageous method of ventilating a wall (in the light of a possible methane hazard occurrence) is the “U” system, in which the methane from the output poses a less serious threat than the methane coming out of goafs and the affected rock mass (Krause, 2009) – of course, provided that there is enough air in the circulating current.

Therefore, it seems advisable to include the flow phenomena occurring in the affected rock mass in the description of the flow phenomena occurring in longwall headings and goafs.

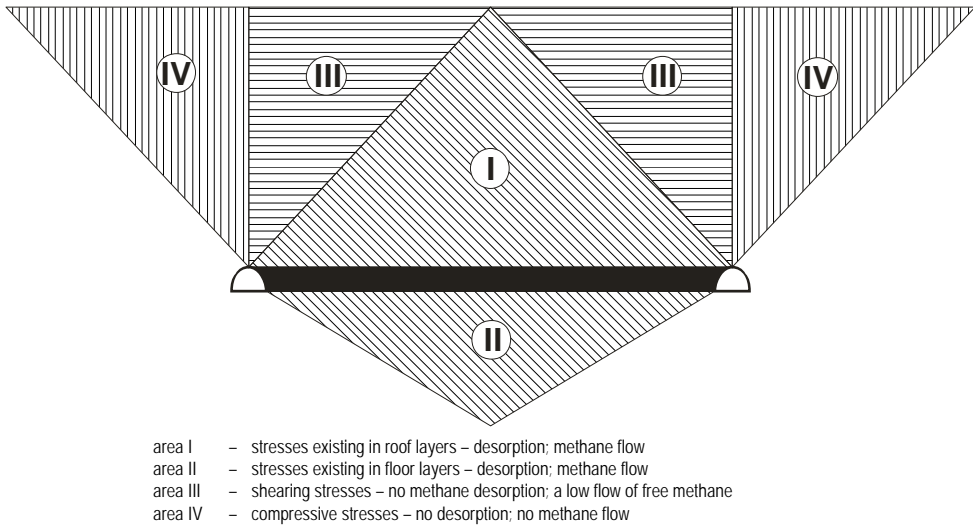


Fig. 1. Stress areas around a longwall heading (Łukowicz, 2012)

The paper presents the results of numerical simulations performed for two geometrical cases: first simulation was based on the calculations for a 100 meter longwall without methane drainage; the second one – on calculations for a 100 meter drained longwall. Both sets concern a U-type ventilated longwall. Adopting the guidelines specified in (Kozłowski & Grębski, 1982; Krause & Łukowicz, 2000; Łukowicz, 2012) – and assuming that the difference in height between the head and tail corner is $\Delta h = 0$ m – we obtain the following main parameters of the computational domain for the examples discussed in this paper (cf. Table 1):

TABLE 1

Main dimensions of the computational domain:

Parameter	Symbol	Unit	Short wall
Longwall length	L	m	100
Seam thickness	m_e	m	2
Range of sorption in the upper area	h_g	m	68,5
Height of the direct cave-in and of the lower desorption area	h_{zb}	m	10
Width of the lower drainage plane	l_d	m	14,6
Width of the upper drainage plane	l_g	m	80

Further, the most representative results of the computations concerning the mass exchange between the affected rock mass and longwall headings are presented, for selected test models.

The discussed geometrical models, as well as all the calculations, were performed with the ANSYS suite of software (for building the models, the GAMBIT program was used; for calculations – the Fluent program).

3. The general description of the constructed geometrical models

The aforementioned sets of wall models were constructed with the following assumptions, common for all cases:

- Seam thickness $m_e = 2$ m,
- An absolute lack of coal remains in goaves,
- The difference in height between the wall inlet and outlet $\Delta h = 0$ m,
- The distributed-type source of methane – off-balance coal seam 0.7 m thick; located 25 m above the floor of the excavated seam,
- The quantities describing the desorption scope in the floor areas were neglected, due to lack of overworked seams.

4. The longwall – no methane drainage version

The model of a 100 meter longwall consists of 20 meter long sections of head and tail gate, the area of goafs reaching 20 m deep behind the casing, and the area of the affected rock mass reaching 67 m above the floor of the longwall headings. Fig. 2 presents the model in question, on which particular areas have been marked.

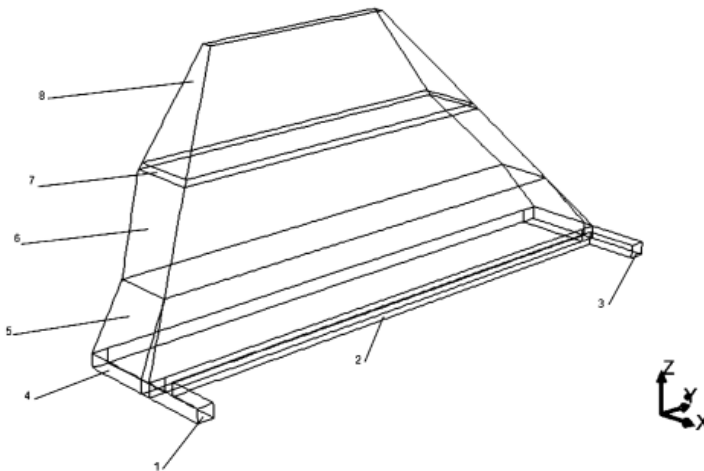


Fig. 2. Geometrical model of the computational area for a longwall – no methane drainage version

1. Inlet – the head gate; 2. Longwall duct; 3. Outlet – the tail gate; 4. Goafs – 20 meters behind the casing;
5. Direct cave-in; 6. High roof fall; 7. off-balance seam; 8. Overlay

The model presented above represents the initial stage of the wall exploitation, during which only a small, 10 meter deep section of the off-balance seam suffers damage due to the wall advance (Fig. 2, position 7).

5. Boundary conditions

Goafs, together with overlayers, were treated as a porous strata, characterized by the particular values of permeability and the material porosity (Młynarczyk & Wierzbicki, 2009) as specified in Table 2.

The average volumetric flow rate of the air in the circulating current was $Q_V = 1400 \text{ m}^3/\text{min}$. The methane-bearing capacity of the off-balanced seam was $3,7 \text{ m}^3\text{CH}_4/\text{Mg}_{\text{CSW}}$.

TABLE 2

Values of porosity and permeability for the sample calculation

Area (Fig. 2)	Porosity ε [-]	Permeability k [m^2]
1	-	-
2	-	-
3	-	-
4	0.35	1e^{-5}
5	0.30	1e^{-6}
6	0.25	1e^{-6}
7	0.25	1e^{-6}
8	0.15	1e^{-7}

The Author considered the non-stationary isothermal flow of the air and methane mixture, in the temperature $T = 300\text{K}$. The boundary conditions for the inlet and outlet surface (Fig. 2, positions 1 and 3, respectively) were determined by means of the differences in the total pressures $\Delta p = 50 \text{ Pa}$ (the difference between the inlet and the outlet of the computational domain).

6. The results of the numerical simulation for a longwall without methane drainage

Unfortunately, obtaining a numerical solution for a seemingly simple geometrical model, like this one, is a long process. This is mostly due to the extent of the computational domain – and significant differences between the speed scales. In goafs, the expected average speed values are ca. 10^{-3} m/s ; they are even smaller in the case of the layers above the direct cave-in; finally, within the circulating current, the average speed of the mix flow is ca. 10^1 m/s . Taking into account the time when the results were obtained, it was assumed that the calculations regarding the non-stationary mass exchange for the discussed wall models were done when the concentration of methane was 1 (or more) percent.

Below, the results of the calculations for the first of the flow cases – no methane drainage version – were presented. The stationary state was obtained after 9 hours (32400 s). Figure 3 shows the distribution of the average speed in a plane parallel to the floor, located 1.2 m above it.

The distribution of speed within the longwall headings reveals two areas where the average speed value is higher: the bottom and top corner area. In the case of a two-time change of the stream momentum caused by a change in the flow direction, this is an absolutely regular phenomenon. Since the distribution of speed shown in Fig. 3 reveals the aforementioned differ-

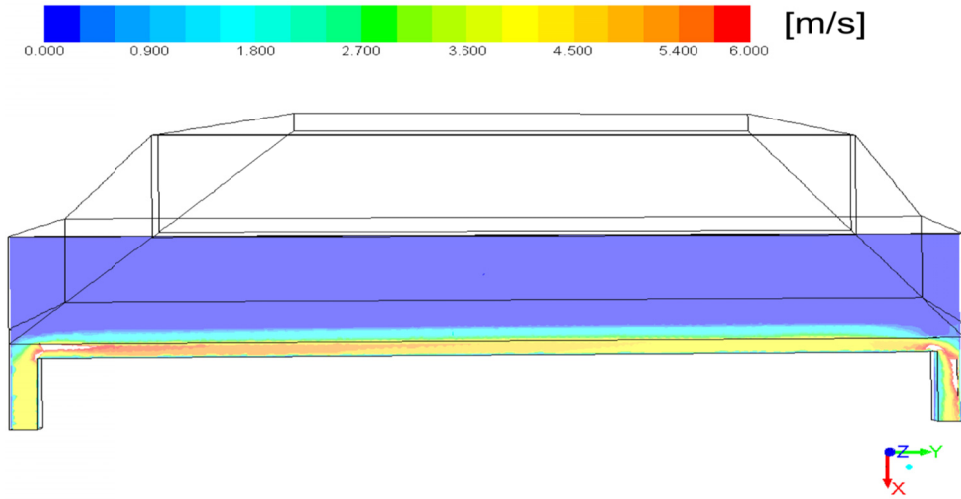


Fig. 3. Distribution of the air flow speed in a plane parallel to the floor, located 1.2 m above the floor

ences in the speed scales between the free flow area (heading) and the flow area in the porous seam (goafs), it was necessary to probe the goafs in order to establish the speed values inside the goafs. Within the U-type ventilated wall, the major trouble spot for the air flow is the head and tail gate corners area. Figures 4a) and 4b) show the probing lines running 1.2 m above the floor, and covering the areas that are of interest from the research perspective.

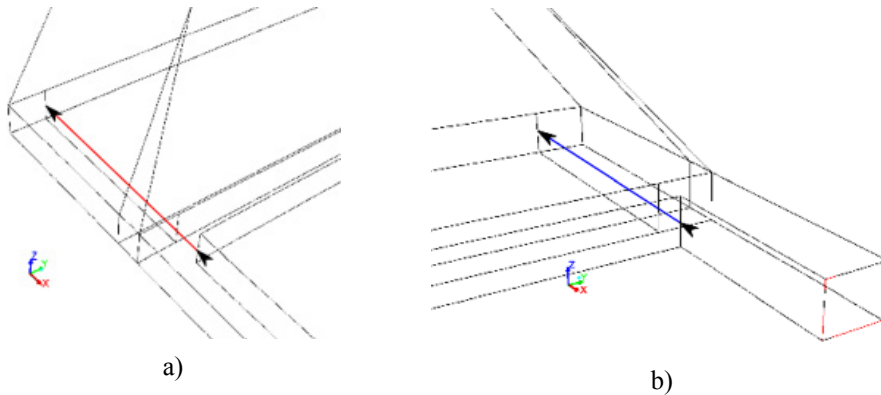


Fig. 4. Probing lines at the inlet a) and outlet b) of the wall

For the probing lines (Figure 4), graphs depicting the changeability of the average speed value down the goafs were created. In Figures 5 and 6, the wall casing is on the abscissa $L = 0$. This means that the values $L < 0$ concern the area of goafs, and the values $L > 0$ – the area of the longwall duct. The red color was used for the profile of the average speed for the probing

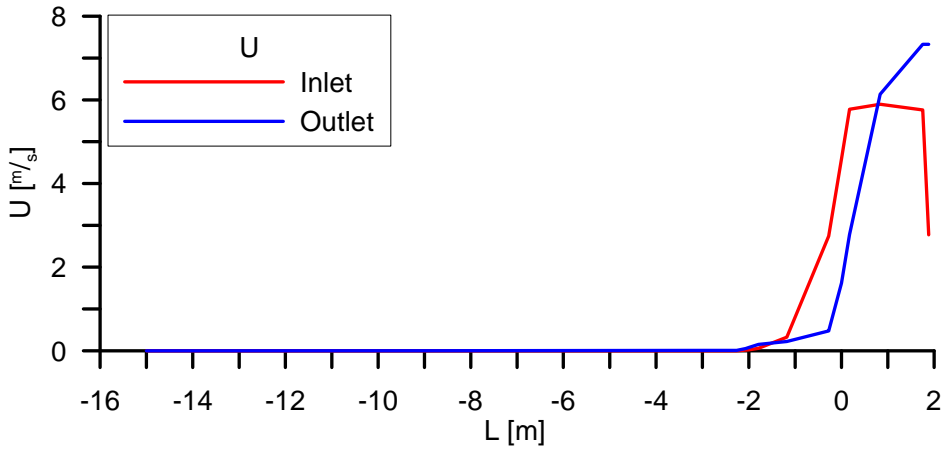


Fig. 5 Distribution of velocity along the probing lines at the inlet and outlet of the wall

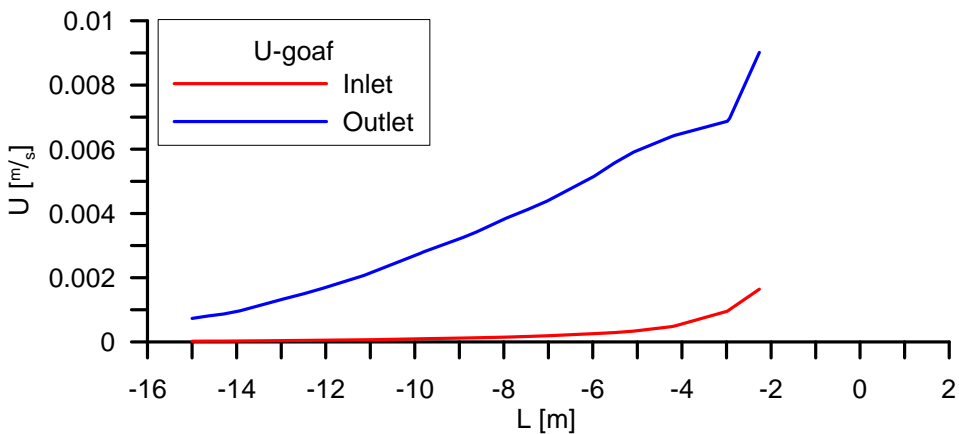


Fig. 6 Distribution of mixture velocity in goafs – the probing lines values

line located at the wall inlet; the blue color – for the profile of the average speed for the probing line at the wall outlet. In order to depict the difference between the speed scales inside the goafs and within the wall duct area, the distribution of the average speed as a function of the distance $L = -2$ m (2 m behind the casing, into the goafs) was presented in Figure 6.

The analysis of the distributions of speed shown in Figures 5 and 6 proves that the difference between the average speed value within the wall duct axis and the furthest point in the goafs is 3 orders of magnitude (0.001 – 6 m/s). The differences between the same phenomenon as observed in the head gate and tail gate corners are, as to the absolute value, negligible.

The differences between the courses of changes in speed in the head and tail corner (particularly those observed within the area of goafs) point to an intense mass exchange between the

goafs and the longwall headings. This is of particular importance when it comes to the presence of methane sources in the affected rock mass.

Figure 7 presents the distribution of the isosurfaces of the three values of the concentration of methane released from the off-balanced seam during the simulation.

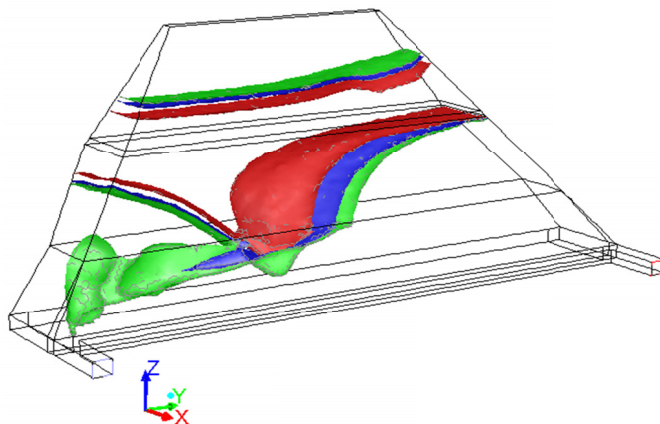


Fig. 7. Isosurfaces of the distribution of methane concentrations in the area of goafs: green color – 1% CH₄, blue color – 2%CH₄, red color – 10% CH₄

The analysis of the shape of the isosurfaces reveals a surprising fact – namely, that methane does not migrate into the longwall headings in an amount sufficient to be considered dangerous, although a source of methane clearly exists here: it is the off-balanced seam affected by exploitation (Fig. 2, position 7).

This observation is confirmed by the graph in Figure 8, which shows the change in the value of methane concentration along the probing lines. As far as the head gate corner is concerned, the peak of the methane concentration value occurs ca. 2 meters behind the casing, whereas in goafs, close to the tail gate corner, methane concentration is at the steady level of ca. 0.1%, and decreases as the distance from the side wall gets shorter. The reason for this was most probably the effective dilution of methane with the air from the circulating current, which – due to the complex porosity and permeability values (cf. Table 1) – could easily penetrate the area of goafs. The case described here is characterized by the fact that the discussed dilution process was considerably stationary in its nature. The latter, after ca. 500 min of the flow duration (cf. the graph in Fig. 9), resulted in the methane concentration increasing to its impassable value of 0.1%, in the outlet section of the top heading.

The presented results of the calculations concerning the exchange of mass for the ventilated short wall with 20 meter goafs, for the adopted parameters of the relaxed rock mass and the volumetric flow rate value within the circulating current, indicate lack of necessity of active drainage of the goafs and the overlaying rock mass.

Thus, for the discussed longwall – as depicted in Fig. 2 – the conditions for the mass exchange between the goafs and the longwall duct are such that they exclude the presence of methane within tail gate corner, for the adopted source.

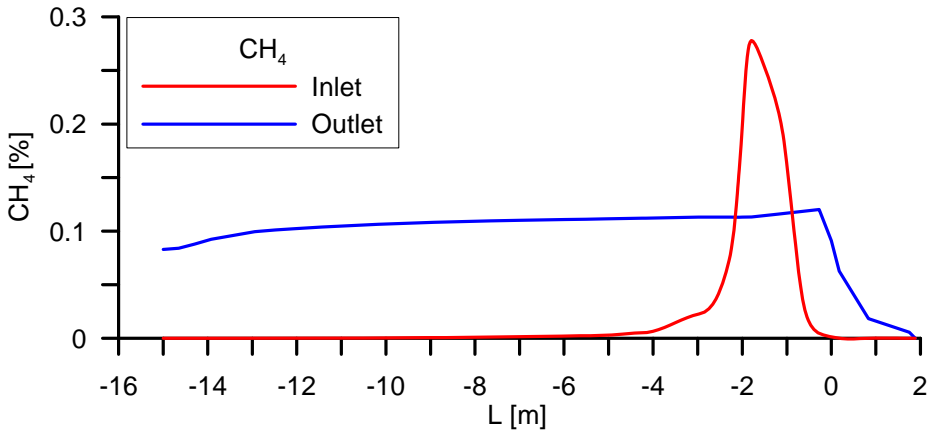


Fig. 8. Change in the value of methane concentration along the probing lines

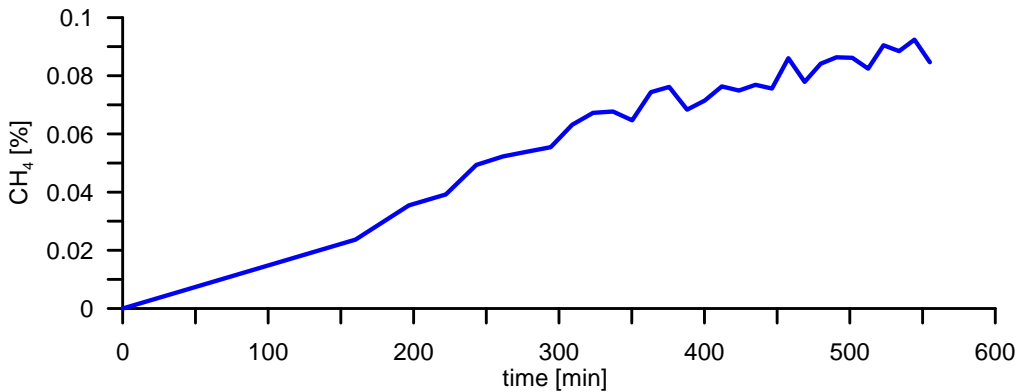


Fig. 9. Concentration of methane within the tail gate

7. The longwall – methane drainage version

In the light of the results obtained for the short wall with goafs reaching 10 meters behind the casing, getting some representative results for the ventilated longwall which would take into account dangerous tail gate corner areas with increased methane concentration called for increasing the volume of the methane source. This was done by expanding the computational domain by means of increasing the area of goafs, together with the overlayers, by 10 m.

Figure 10 presents the new geometrical model, with additional 12 methane drainage holes placed in affected rock mass, near the tail gate.

In Figure 10, the expanded area of the computational domain (extra 10 meter goafs section) was shaded. The distribution of the introduced layers, as well as their flow parameters (porosity, permeability), are identical with the distribution and flow parameters of the original model (Table 2). The volumetric flow rate for the air in the circulating current was $Q_V = 1400 \text{ m}^3/\text{min}$,

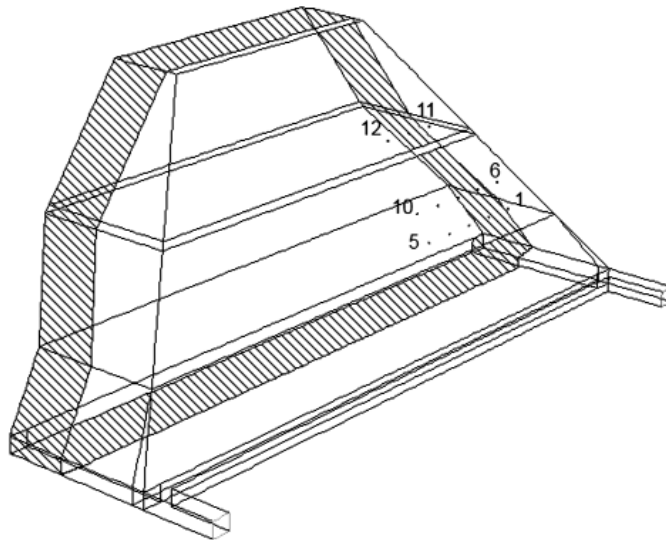


Fig. 10. longwall – methane drainage version. The expanded geometrical model

as was the case with the previous model. What did change, however, was the methane-bearing capacity of the off-balanced seam, which was $5,2 \text{ m}^3 \text{CH}_4 / \text{Mg}_{\text{G}_{\text{CSW}}}$.

Just like in the previous example, the question considered was the non-stationary isothermal flow of the air and methane mixture at the temperature $T = 300\text{K}$. The total pressure drop at the inlet and outlet was $\Delta p = 50 \text{ Pa}$.

The drainage holes were arranged in the desorption plane according to the relevant data in (Fluent User..., 2011), which specifies the optimum spatial arrangement of the holes (cf. Figure 11).

The outgassing process was carried out under the given depression of 200 Pa, in all the holes (o1 – o12 – Fig. 10). The negative pressure value concerned the inlet of the drainage hole in the affected rock mass.

8. The results of the numerical simulation for methane drainage version

The results of the numerical simulation, presented below, describe the distribution of the values of methane concentration in the affected rock mass and within the area of longwall headings after 9 hours (32,400 s).

The depression in drainage holes, together with the negative pressure at the outlet of the tail gate, results in a significant distortion of the concentration isosurfaces presented in Figure 12.

This effect is particularly visible in the vicinity of the right desorption plane (as seen from the perspective of the tail gate corner). The lower part of the isosurfaces 1, 2 percent (as seen from the perspective of the off-balanced seam) and 10 percent (marked with green, blue, and red color, respectively) moves visibly towards the upper corner, whereas the upper part of the isosurfaces assumes a curved, but, at the same time, more regular shape.

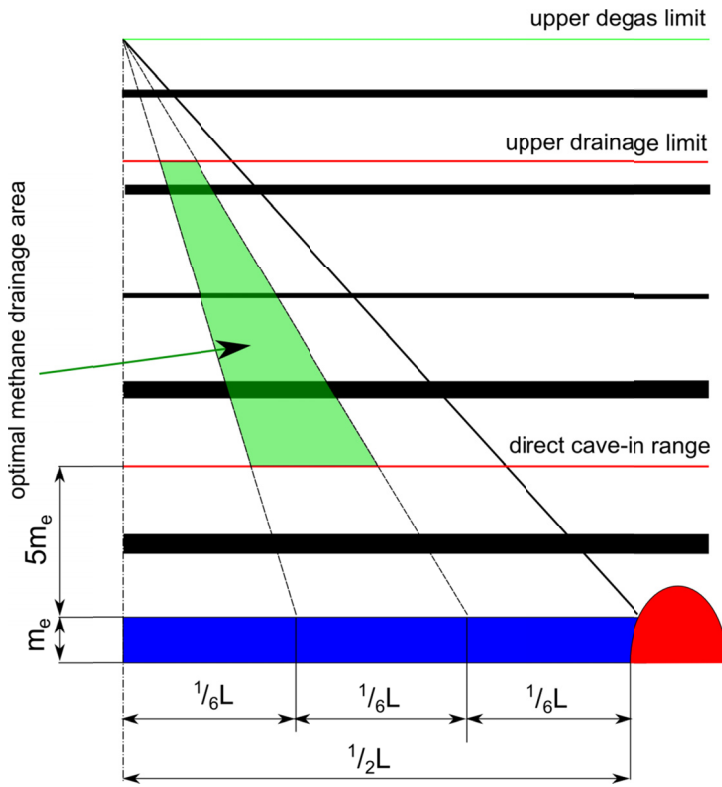


Fig. 11. Determining the optimal methane drainage area (Fluent User..., 2011)

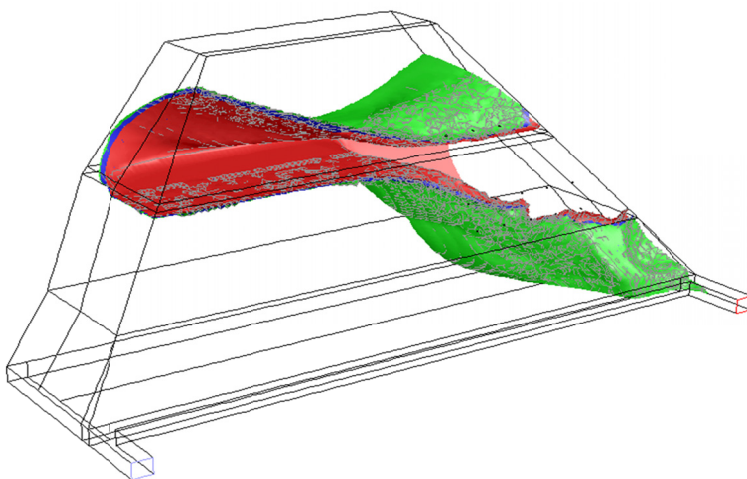


Fig. 12. Isosurfaces of the distribution of methane concentration values within the goafs and the longwall headings – methane drainage version

The regularity of the curvature of the upper isosurfaces will become more comprehensible if we analyze the distribution of the current lines shown in Figure 13. Such an analysis clearly shows that some of the drainage holes participate in the active drainage of the air and methane mix, whereas some others – o4, o5, as well as o9, o10, o11, and o12 – draw in the air coming from as far as the lower abandoned heading.

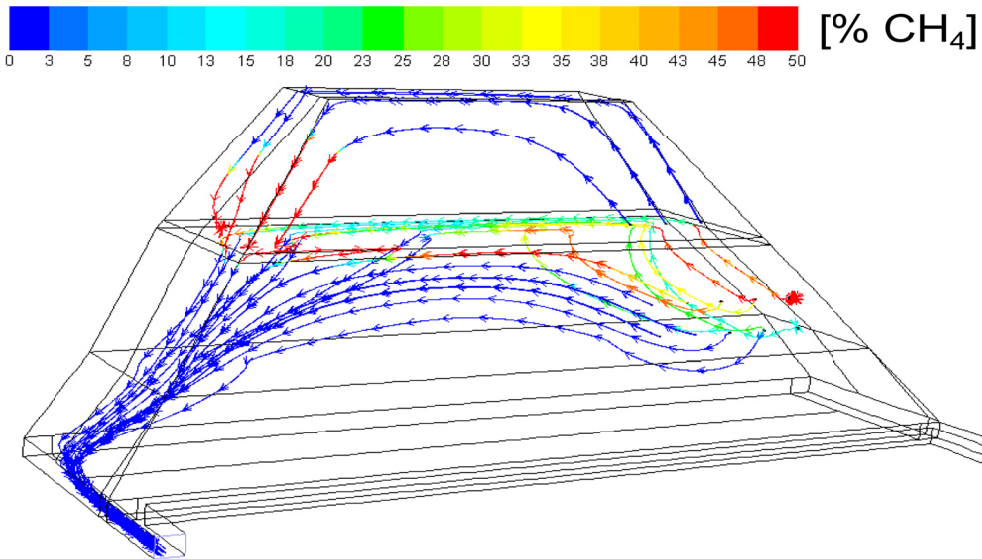


Fig. 13. Distribution of the stream lines – a longwall, methane drainage version

Thus, the methane drainage process becomes less effective; the drainage holes participating in the drainage of the air and methane mixture are characterized by lower concentration values.

Figure 14 presents a graph depicting the changeability of the methane concentration value in the drainage holes taking part in the process in question. The holes in the front row – o1, o2, and o3 – drain the mix with the lowest methane content. This is probably due to the interaction with adjacent holes o4 and o5, which drain the mix with slight methane content. A similar situation occurs in the case of the holes in the second row, i.e. o6, o7, and o8. Here, the holes that disturb the functioning of the whole drainage system are the upper ones – o9, o10, o11, and o12.

9. Summary and conclusions

The paper presents the results of numerical simulations in 3D performed for two test, U-type ventilated longwalls. The cases in question are characterized by fairly simple geometry and homogenous boundary conditions. Although certain indispensable simplifications (mainly geometrical ones) were introduced, the discussed longwall models still proved to be fairly consistent with the overall body of knowledge concerning mining, as well as with the mining practice. Thus,

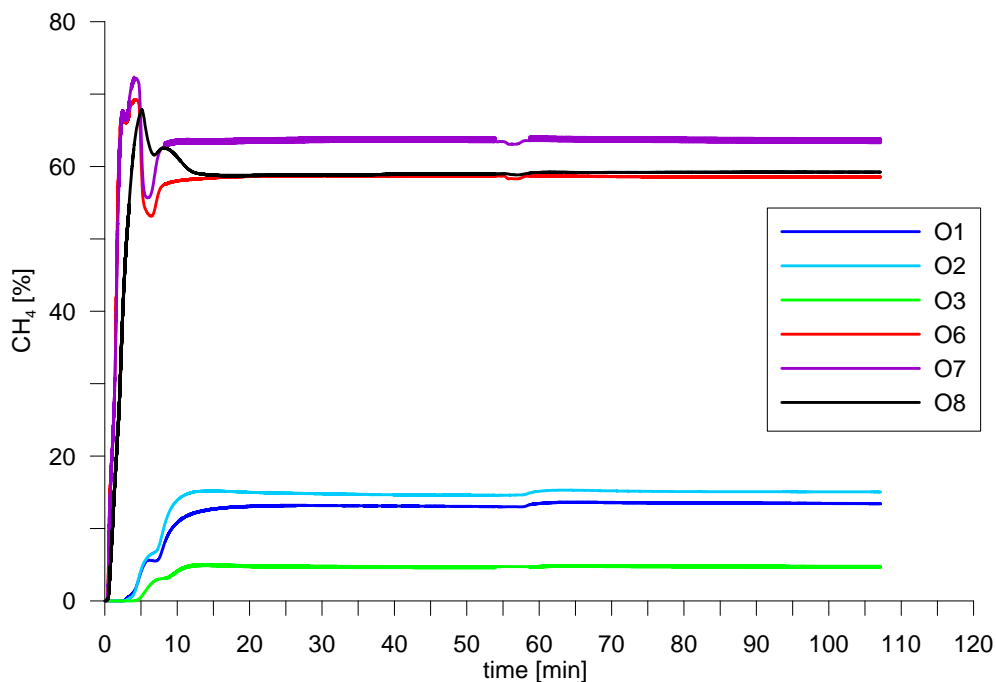


Fig. 14. Methane concentration in drainage holes

as test cases, they provide a good basis for calculations performed for walls more similar to real ones (the length of a wall being $L > 100$ m).

At this point, it is necessary to emphasize several factors that need to be taken into consideration while applying certain solutions of the numerical fluid mechanics in issues related to safety and efficiency of extraction:

- numerical analyses are performed mostly under ideal conditions. In reality, disturbing the functioning of any of the drainage holes (by tightening or shearing it) may result in loss of control over the ventilation conditions within the wall;
- the basic problem is the time of the analysis. It is advisable to adopt such simplifying assumptions that will make it possible to shorten the simulation time dramatically; however, with no detriment to the quality of the obtained results;
- the many factors influencing the effectiveness of the mass exchange in the discussed system make the whole question a very complicated one. The presented results indicate that results as such can be more accurate when there is a sufficient number of the input data concerning the distribution of the geological layers, their porosity, coefficients of permeability and methane-bearing capacity;
- finally, particular attention should be paid to the selection of the values of the parameters of permeability and porosity of the goafs and overlay material. This is due to the fact that they have a significant influence on the rate of the mass exchange – the greater the porosity and permeability, the higher the methane concentration behind the casing and in the tail gate corner.

Acknowledgments

The paper was prepared under the Strategic Project Task 4, Subtask 4.3.2 entitled “Improving the efficiency of rock mass methane drainage under conditions of high concentration of mining in underground coal mines” No. SP/K/4/159840/12 supported by the National Centre for Research in Warsaw, Poland.

References

- Dziurzyński W., Krach A., Krawczyk J., Palka T., 2009. *Metoda regulacji elementów sieci odmetanowania z wykorzystaniem symulacji komputerowej* Arch. Min. Sci., Vol. 54, No. 2, p. 159-188.
- Fluent User Guide, Ansys Inc. 2011.
- Kozłowski B., 1972. *Prognozowanie zagrożenia metanowego w kopalniach węgla kamiennego*. Katowice, Wyd. Śląsk.
- Kozłowski B., Grębski Z., 1982. *Odmetanowanie górotworu w kopalniach*. Katowice, Wyd. Śląsk.
- Krause E., Łukowicz K., 2000. *Dynamiczna prognoza metanowości bezwzględnej ścian* (poradnik techniczny) Wyd. GIG, str. 36.
- Krause E., 2009. *Ocena i zwalczanie zagrożenia metanowego w kopalniach węgla kamiennego* Prace GIG Studia-Rozprawy-Monografie Nr 878 Katowice 2009
- Łukowicz K., 2012. *Wyznaczenie parametrów modelu numerycznego rejonu ściany w aspekcie prowadzenia odmetanowania dostosowanych do warunków górniczo-geologicznych*, opracowanie dla IMG-PAN, nie opublikowane.
- Młynarczuk M., Wierzbicki M., 2009. *Stereological and profilometry methods in detection of structural deformations in coal samples collected from the rock and outburst zone in the “Zofiówka” Colliery*, Arch. Min. Sci., Vol. 54, No. 2, p. 189-201.

Received: 12 January 2013